Mapping the Dynamics of Visual Feature Coding: Insights into Perception and Integration

Tijl Grootswagers[1*^], Amanda K. Robinson[2*], Sophia M. Shatek[3], Thomas A Carlson[3]

[1] The MARCS Institute for Brain, Behaviour and Development, Western Sydney University, Sydney, Australia
[2] Queensland Brain Institute, The University of Queensland, Brisbane, Australia
[3] School of Psychology, The University of Sydney, Sydney, Australia
* Equal contribution ^ t.grootswagers{at}westernsydney.edu.au

Abstract

The basic computations performed in the human early visual cortex are the foundation for visual perception. While we know a lot about these computations from work in non-human animals, a key missing piece is how the coding of visual features relates to our perceptual experience. To investigate visual feature coding, interactions, and their relationship to human perception, we investigated neural responses and perceptual similarity judgements to a large set of visual stimuli that varied parametrically along four feature dimensions. We measured neural responses using electroencephalography (N=16) to 256 grating stimuli that varied in orientation, spatial frequency, contrast, and colour. We then mapped the response profiles of the neural coding of each visual feature and their interactions, and related these to independently obtained behavioural judgements of stimulus similarity. The results confirmed fundamental principles of feature coding in the visual system, such that all four features were processed simultaneously but differed in their dynamics, and there was distinctive conjunction coding for different combinations of features in the neural responses. Importantly, modelling of the behaviour revealed that every feature contributed to perceptual experience, despite the untargeted nature of the behavioural task. Further, the relationship between neural coding and behaviour was evident from initial processing stages, signifying that the fundamental features, not just their interactions, are crucial for perceptual experience. This study highlights the importance of understanding how feature coding progresses through the visual hierarchy and the relationship between different stages of processing and perception.

Introduction

The initial stages of human visual processing involve basic computations that form the foundation of our perception of the world. Neural populations within the primary visual cortex (V1) are responsible for encoding the basic features of a visual stimulus (Hubel, 1988; Hubel and Wiesel, 1959). Within V1, neurons are selective for multiple features within the visual scene, including edge orientation, spatial frequency, contrast, and colour. Yet encoding of features is not confined to V1. Basic feature dimensions also have distinct responses in higher visual areas, for example colour coding in V4 (Brouwer and Heeger, 2009). Indeed, feature-specific coding has been documented throughout the visual system (Van Essen and Gallant, 1994; Zeki et al., 1991). However, a key missing piece in the literature concerns how visual feature coding relates to perceptual experience. For example, which features have distinct effects on perception, and does the encoding strength of a feature predict its perceptual weighting? Obviously, answering these questions are not possible in monkeys or cats, and human neuroimaging has mainly focused on low-level perceptual psychophysics. Understanding how features are coded across successive stages of processing can provide insight into the computations that transform visual input into perceptual experience.

Human neuroimaging methods with high temporal resolution have been increasingly applied to characterise the dynamic processes underlying visual feature coding in the brain. Orientation, spatial frequency, colour, and contrast information can separately be decoded from neural signals as early as 50 ms following a visual stimulus, and different features appear to have distinct temporal profiles (Cichy et al., 2015; Groen et al., 2022; Hajonides et al., 2021; Hermann et al., 2022; Ramkumar et al., 2013; Rosenthal et al., 2020; Teichmann et al., 2020, 2019). These findings highlight the potential of time-resolved neuroimaging methods not only for tracking the coding of visual features in the brain, but also for revealing how coding changes over time. Temporal profiles are particularly informative in showing when feature coding is maximal, indicating the time that the most feature information can be extracted from the brain. However, many human neuroimaging studies focus on only one or two visual features, making it difficult to directly compare temporal profiles across experiments with different methods.

Perceptual experience relies on combining features into a single percept. The binding problem refers to the challenge of combining information from separate neural populations from different modalities (e.g., sound and sight) or different features (e.g., colour and motion) into a unified representation. This problem may also apply within the same neural populations (Zeki, 2020). For example, the observation that orientation and colour are both coded in V1 (Friedman et al., 2003) does not imply that they are integrated together at this stage. Neural populations that code for multiple features could reflect an efficient feature coding-scheme and/or reflect coding of conjunctions (i.e., specific combinations of features). Studies using fMRI have shown plausible conjunction coding throughout the visual system, such as colour and motion (Seymour et al., 2009), colour and form (Taylor and Xu, 2022), and spatial frequency and form (Cowell et al., 2017). This work showed that the conjunction codes were different from the individual feature codes, but did not elucidate when the conjunction codes emerged. One possibility is that conjunction coding reflects feedback or recurrent processes, not early feedforward

computations. Resolving these possibilities requires high temporal resolution population-level neural responses to reveal the timing of individual features compared to conjunctions.

In addition to understanding how individual visual features (and combinations of these features) are encoded in the brain, a critical aspect that has remained a challenge is understanding how encoding of individual features informs our perceptual experience of the stimuli. For example, are behaviourally relevant features more strongly coded in the brain? A recent development in the field has been to explore more deeply the extent to which neural coding informs conscious perception. High level information (e.g., object category) has been shown to be predictive of behaviour (e.g., Carlson et al., 2014; Grootswagers et al., 2018; Mur et al., 2013; Ritchie et al., 2015). Wardle et al., (2016) found that even for simple visual patterns, observer ratings of perceptual similarity are a good predictor of neural responses (Wardle et al., 2016). It seems quite clear that neural responses to complex information such as form and category drive behaviour, but is the same true for the first stage of processing in our visual system?

In this study, we aimed to map temporal response profiles, interactions, and behavioural relevance of basic visual features. We measured neural responses using electroencephalography (EEG) while participants viewed 256 oriented gratings that varied on four feature dimensions: orientation, spatial frequency, colour, and contrast. We used a highly efficient rapid presentation design where stimuli were presented in fast sequences at 6.67 Hz or 20 Hz to differentially mask the images, restricting processing time/capacity in the 20Hz condition (Robinson et al., 2019). In addition, we collected independent behavioural judgements of perceptual similarity on these gratings (Figure 1). We sought to resolve three questions: (1) What are the neural dynamics of basic feature dimensions in the human brain? (2) How do different features interact? (3) How do feature-related neural responses relate to observers' perceptual experience? Our results reveal overlapping but distinct dynamics of the coding of features and conjunctions in the human brain, and demonstrate strong evidence that feature coding drives perceptual experience.

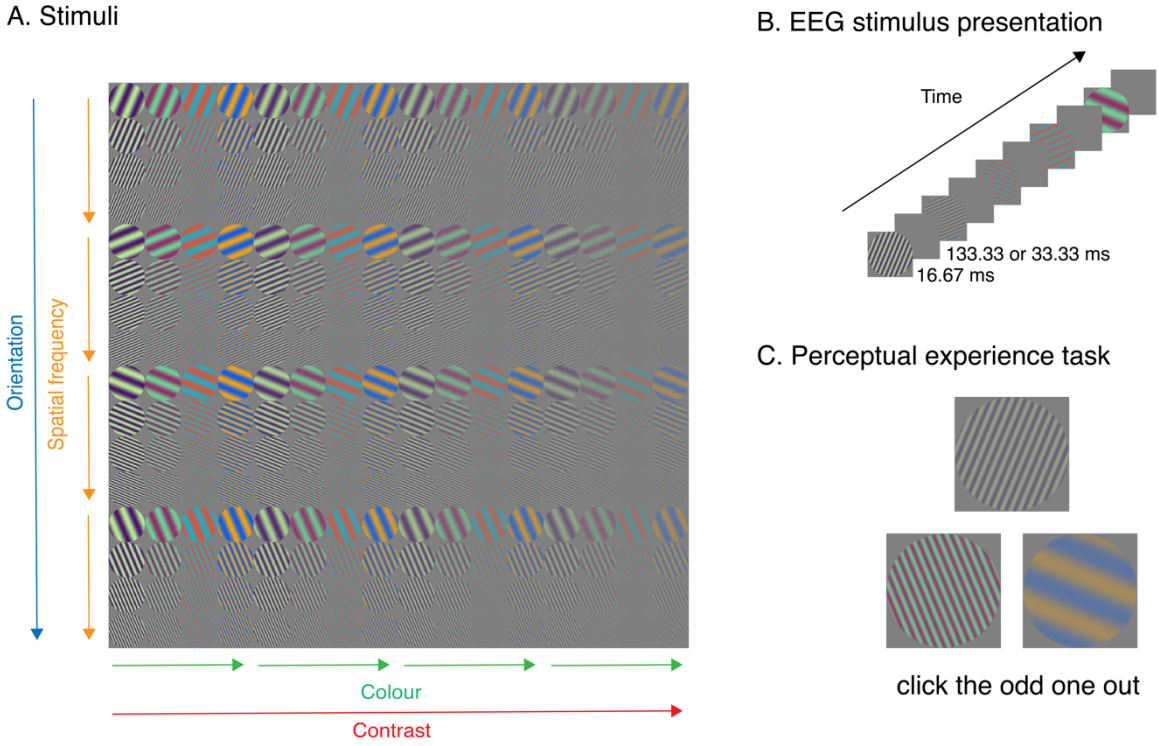

Figure 1. Experimental design. A) Stimuli were 256 oriented gratings that differed across four dimensions: spatial frequency, colour, orientation, and contrast. B) Example trials for EEG experiment. Stimuli were presented for one frame (16.67 ms) in sequences at 6.67 Hz (133ms ISI; 150ms SOA) or 20 Hz (33ms ISI; 50ms SOA). C) Example trials for the perceptual experience task. Participants chose the stimulus that looked the most different (odd-one-out).

Results

Dynamic visual feature coding in the EEG signal

Our results showed highly overlapping dynamic information for orientation, spatial frequency, colour, and contrast (Figure 2A). Using multivariate pattern analyses to "decode" different levels of each feature (e.g., different orientations, different contrast levels), we observed featural information in response to images at both 6.67Hz and 20Hz. Group statistics of decoding onset (as indexed by first three consecutive time points BF>10) indicated that all four features could be discriminated in the neural signal beginning from <90ms, at very early stages of processing (Figure 2A, Table 1). These times are consistent with early visual processing, likely beginning in the primary visual cortex. Notably, 95% confidence intervals of the onset times for the 6.67 Hz frequency were similar for spatial frequency, colour and contrast, indicating highly overlapping coding of these features in time. Orientation coding was lower overall, and that corresponded with a later onset of decoding, but it was still decodable in parallel with the other features. Contrast information peaked earliest, followed by spatial frequency and colour, and then orientation. Onset times were slightly later for colour and contrast in the 20Hz condition relative to the 6.67Hz condition, but peak times for decoding of each feature was nearly identical for the two presentation conditions, suggesting that feature processing was not affected by masking. Time generalisation results revealed two pronounced stages of processing per feature (Figure 2B), with above-chance generalisation for training and testing on similar time points, and below-chance decoding for generalisation from one stage to the other (e.g., training on 100ms and testing on 180ms, and vice versa). These two-stage processing dynamics are consistent with previous work (Carlson et al., 2013; King et al., 2016; Moerel et al., 2022a) and could reflect early stage feedforward and subsequent higher level recurrent processing (King and Dehaene, 2014). Each feature exhibited slightly different patterns of generalisation suggesting the involvement of different neural populations. Together, these results indicate that orientation, spatial frequency, colour, and contrast have different coding dynamics, but that these processes operate in parallel, and the dynamics are highly conserved across different presentation conditions.

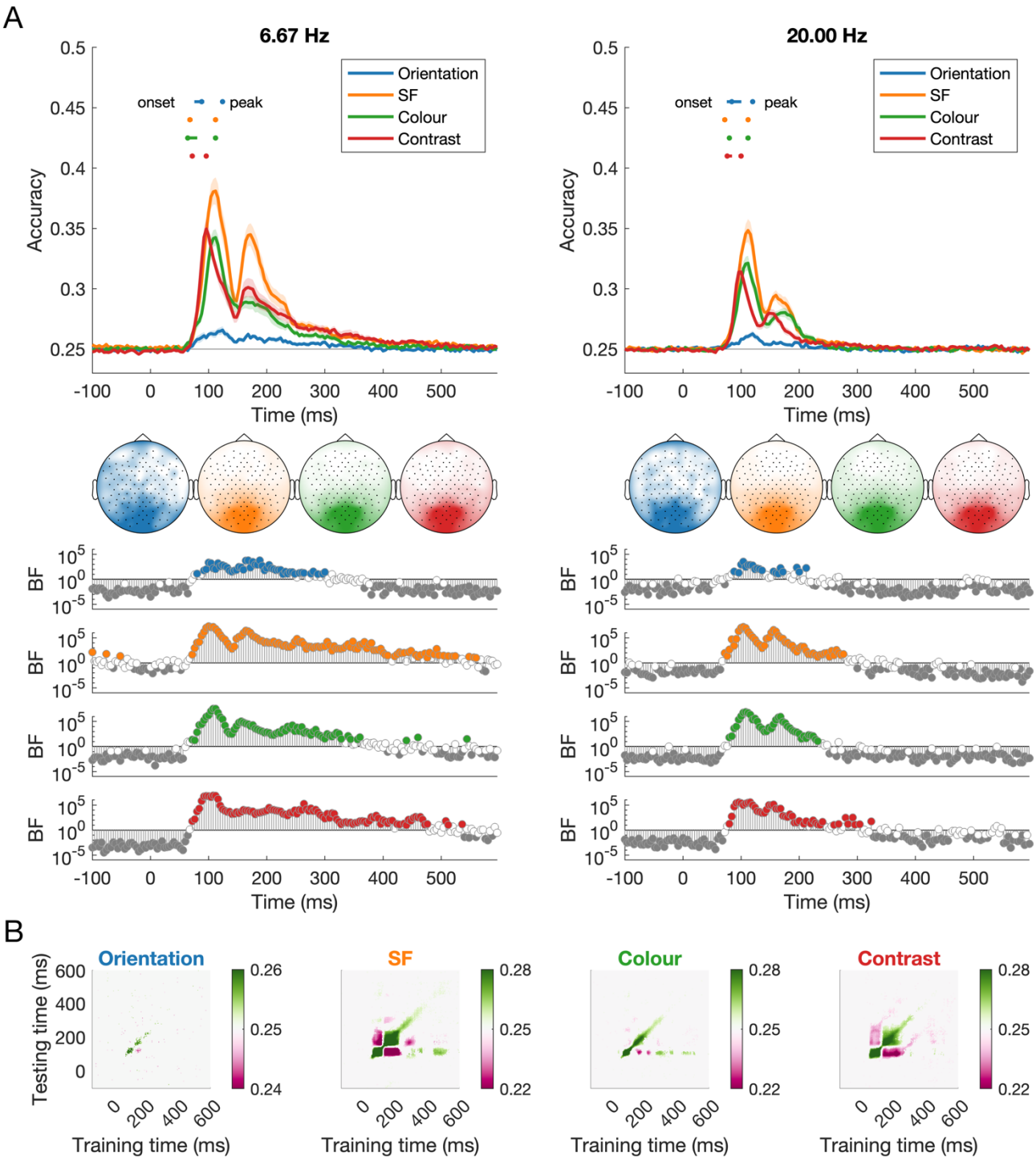

Figure 2. Dynamics of visual coding for orientation, spatial frequency, colour, and contrast at different stimulus presentation rates. A) The time course of decoding accuracy at 6.67Hz and 20 Hz presentation rates. Confidence intervals for onsets and peaks of individual features are plotted above the decoding traces. The head maps show the channel clusters with the highest feature information at the peak of decoding, based on results from a channel searchlight analysis. Bayes Factors for classification evidence compared to chance (0.25) are plotted below. Coding peaked in order from contrast, then colour and spatial frequency, followed by orientation. The dynamics of feature coding were very similar regardless of presentation rate, though there was numerically higher classification accuracy for 6.67Hz compared to 20Hz. B) Time x time generalisation analyses for 6.67Hz condition show different above-chance and below-chance dynamics for each feature.

Table 1. Timing of onset and peak of EEG decoding for features orientation, spatial frequency (SF), colour, and contrast, interactions between features, and for the correlation between EEG decoding and behaviour. Cells with no values indicate no reliable onset time could be extracted. Temporal resolution was 4ms, and 95% confidence intervals are shown in square brackets.

		Onset time (ms)		Peak time (ms)	
	Feature	6.67Hz	20Hz	6.67Hz	20Hz
Individual	Orientation	88 [76-92]	84 [76-100]	124 [124-124]	120 [120-120]
	SF	68 [64-72]	72 [68-72]	112 [108-112]	112 [112-112]
	Colour	64 [64-80]	80 [80-80]	112 [108-112]	112 [108-112]
	Contrast	72 [68-72]	76 [76-84]	96 [96-96]	100 [96-100]
Interactions	Colour x contrast	88 [84-88]	96 [96-96]	148 [100-148]	100 [100-100]
	SF x contrast	84 [84-84]	88 [88-88]	172 [92-176]	104 [104-104]
	SF x colour	80 [76-80]	88 [84-100]	120 [120-124]	124 [124-124]
	Orientation x contrast	-	128 [84-160]	100 [96-124]	116 [116-328]
	Orientation x colour	-	-	168 [168-168]	108 [80-192]
	Orientation x SF	104 [100-124]	120 [96-120]	136 [136-184]	112 [112-120]
	Behaviour	80 [80 84]	84 [80 88]	108 [108 108]	112 [112 112]

Interactions and conjunctions of feature coding

Next, we were interested in how feature coding varied as a function of the stimulus content. We decoded orientation, spatial frequency, colour, and contrast for each level of the other features, for example decoding colour separately for each orientation (22.5, 67.5, 112.5 and 157.7 degrees). This analysis revealed interesting interactions that can be assessed by peak decoding accuracy (Figure 3). Notably, colour and contrast decoding decreased as spatial frequency decreased. Furthermore, spatial frequency and contrast decoding varied considerably depending on the colour of the stimuli, with higher decoding for the bluer/redder versus greener/purpler stimuli. Spatial frequency, but not colour, varied by contrast, such that the highest contrast resulted in the highest decoding accuracy. Classification of each feature did not vary consistently as a function of orientation, and orientation coding did not vary reliably across the levels of the other features. Note that although orientation coding was much lower overall, classification appeared above chance for each subset, showing that orientation information was reliably present in the neural responses despite its low signal (Figure 3, top row). Although Figure 3 shows only 6.67Hz results, the same trend in results was seen at both presentation rates (see Supplementary Material).

We used a different approach to investigate feature conjunction coding. The visual system is considered a hierarchy, beginning with independent visual feature processing (e.g., colour red, horizontal line) that ultimately seems to form a unitary percept (e.g., red line). Understanding the scale and timing

at which features become jointly processed can help shed light on how features are bound together in the visual system. To do this, we decoded groups of stimuli that each had the same absolute features, but varied in their feature *combinations*. We assessed conjunctions of two features at a time, using two levels of each feature in different combinations (see Figure 4A for the logic of this analysis). For example, to look at the conjunction of orientation and colour, one analysis classified between *orientation1/colour1* AND *orientation3/colour4* (Class A) VERSUS *orientation3/colour1* AND *orientation1/colour4* (Class B). Each analysis included all experimental stimuli with those features (e.g., across all spatial frequencies and colours), so there were 32 stimuli per class (Figure 4B). For each of the 6 feature combinations (colour × contrast, SF × contrast, SF × colour, orientation × contrast, orientation × colour, orientation × SF), there were 36 possible stimulus level combinations that were classified (e.g., 1/1 and 2/2 VS 1/2 and 2/1, 1/4 and 3/2 VS 1/2 and 3/4, etc). From these 36 analyses, the mean was calculated and compared to chance level of 50%. Because the classes could not be distinguished based on any one feature alone, above chance classification for this analysis reflects unique neural responses to the *combinations* of different pairs of features, indicating the presence of feature binding.

Figure 4C shows the dynamics of feature conjunction coding for each combination of features for the 6.67Hz presentation rate. These analyses showed reliable decoding for colour × contrast, spatial frequency × contrast, spatial frequency × colour and orientation × spatial frequency, reflecting specific neural processes for binding of these feature combinations. Decoding was reliable from early stages of processing, and different dynamics were evident for different feature combinations. Orientation × contrast, and orientation × colour did not show reliable above-chance decoding for any prolonged amount of time, though there were time points after 90ms for which there was uncertain evidence in support for the null or alternate hypotheses, indicating a lack of power for these analyses. There was a reliable progression in interaction coding onset, with the earliest coding for SF × colour, then SF × contrast and colour × contrast and finally orientation × SF. Notably, these onset times were later than coding of their respective individual features, indicating that feature binding was a subsequent stage of processing after individual feature coding, more than 12ms later. Though the peak times confidence intervals were quite large for some conjunctions, it was particularly evident for colour × SF that the peak occurred 8-12ms later than the peak of information for each feature alone, providing further evidence of distinct neural populations coding for the conjunction of features compared with individual featural coding.

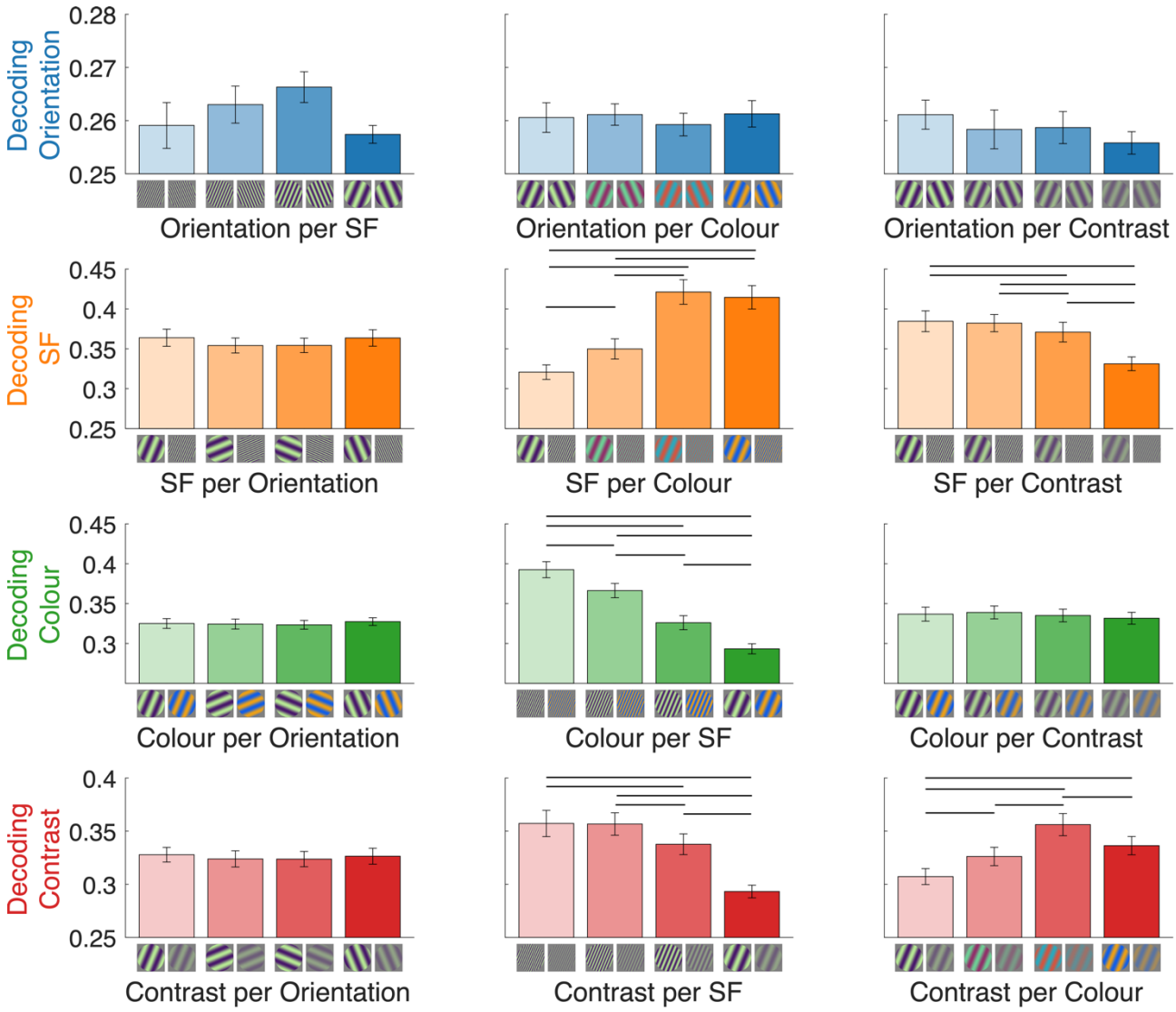

Figure 3. Interactions between coding of different features at 6.67Hz. Mean peak decoding accuracy for orientation, spatial frequency, colour and contrast (rows) according to each level of the other features (columns). Images below each bar depict two example stimuli that were decoded in that analysis. Lines above the bars mark conditions that differ reliably in decoding accuracy (BF $>$ 10). Note the different y-axis scales per row. Y-axis starts at chance level, 0.25.

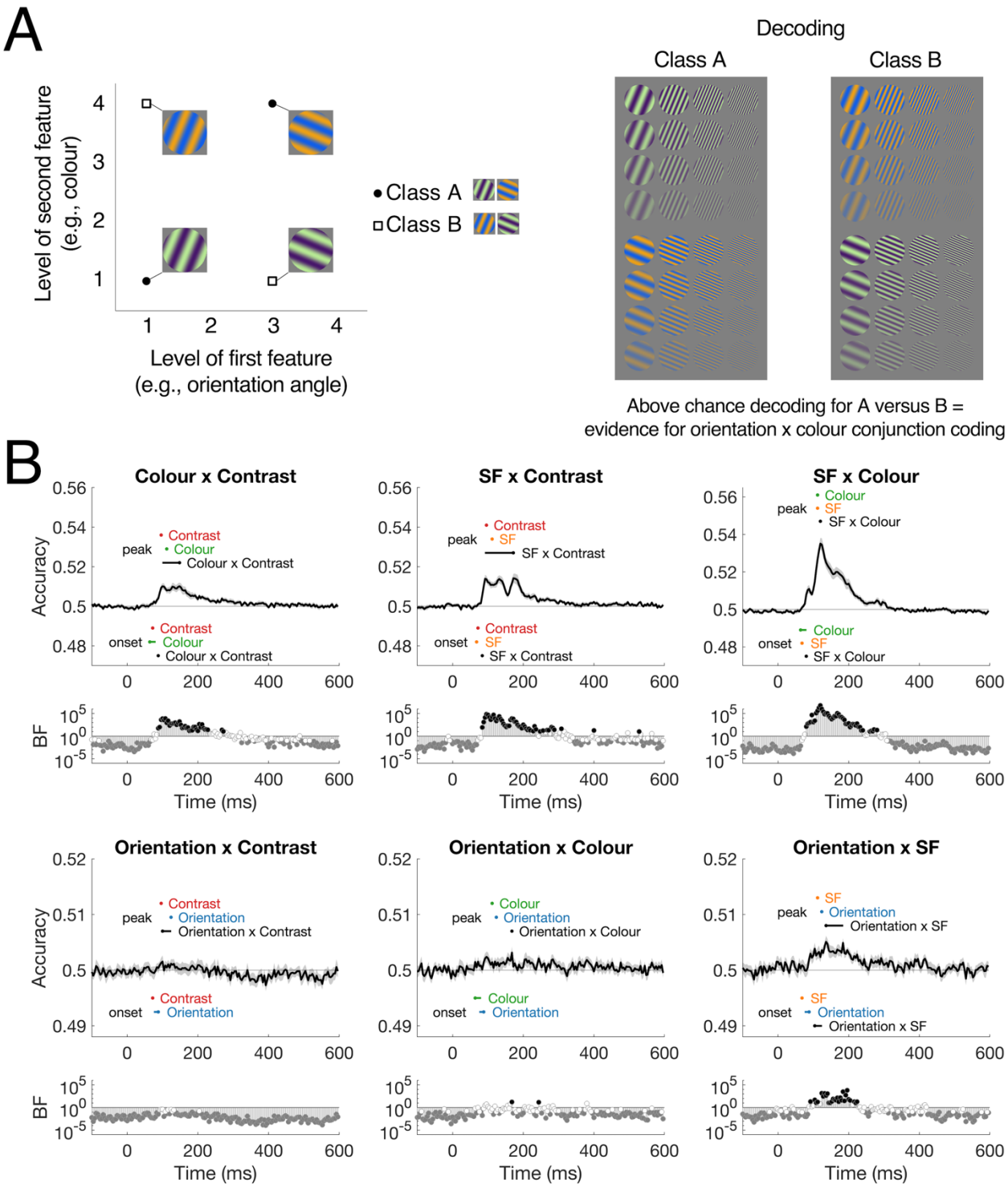

Figure 4. Feature conjunction analyses. A) Logic for the conjunction decoding analysis. Decoding classes came from two levels of two different features (e.g., contrast and orientation), so that each class could not be separated by differences in each feature alone. Classification was performed on groups of stimuli that together contained the same visual features (e.g., specific contrast and orientation) but varied on feature combinations. In this example, both classes contain two contrast levels and two orientations (and four colours and four SFs), so the only way to distinguish between them is by a neural response to the conjunction of contrast and orientation. B) Dynamics of feature conjunction coding for each feature combination. Onsets and peaks of individual features and conjunctions are plotted with 95% confidence intervals; onsets are below the chance level and peaks are above. Bayes Factors below each plot reflect the evidence for above-chance decoding; black circles are BF>10 and grey circles are BF<0.1. All results shown from 6.67Hz presentation rate. Note the different y-axis scales per row.

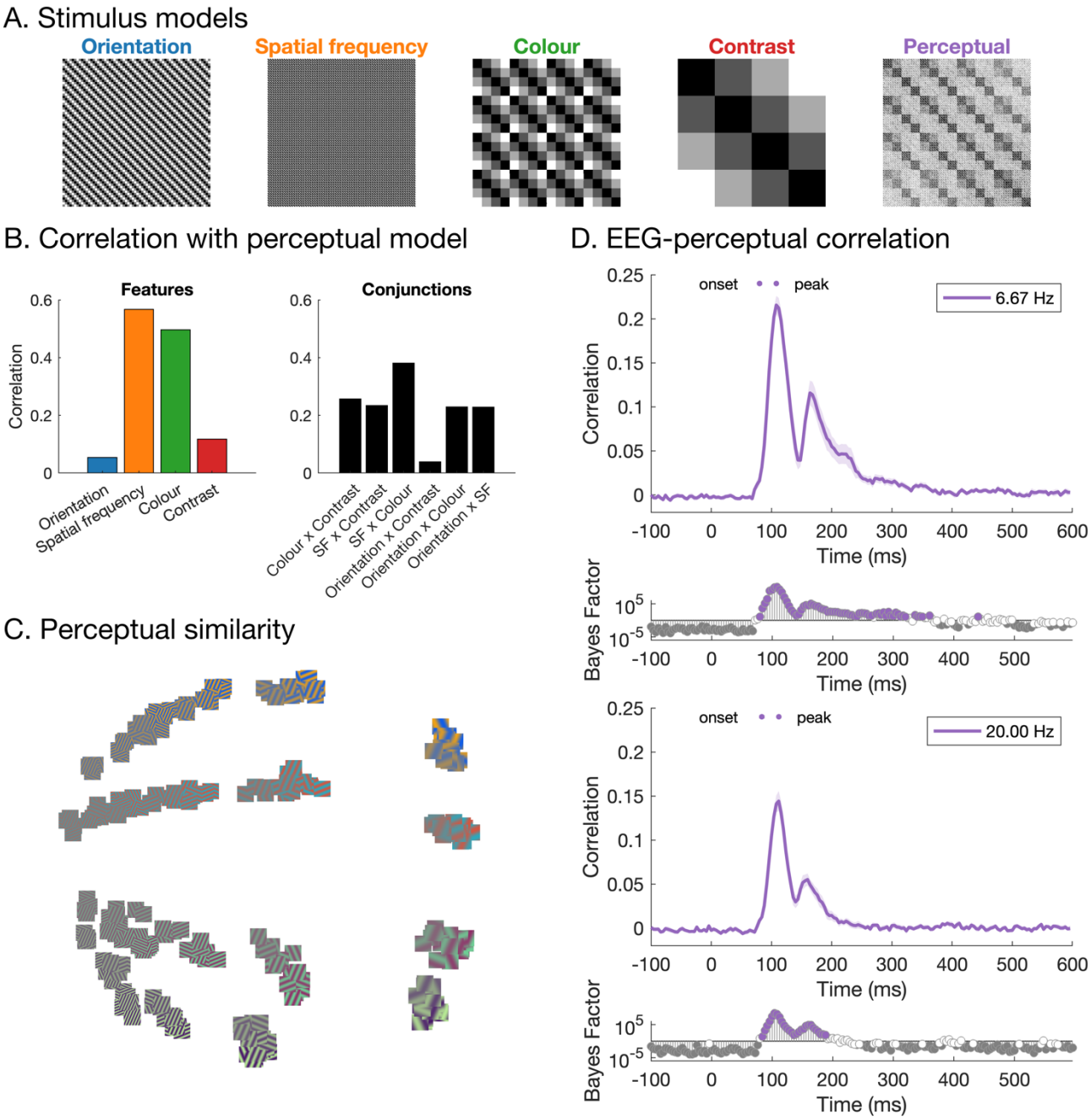

Figure 5. Representational similarity analysis. A) Models (representational dissimilarity matrices) based on stimulus orientation, spatial frequency, colour and contrast, and the perceptual model which was based on perceptual similarity judgements. B) Correlations between the feature models (and their conjunctions) and the perceptual similarity model. C) Similarity between stimuli based on perceptual similarity judgements, plotted using multi-dimensional scaling. The distance between stimuli reflects perceptual similarity, where images that are closer together tended to be judged as more similar perceptually. D) Correlations between neural RDMs and the behavioural model for 6.67Hz and 20Hz presentation rates. From early stages of processing, there are high correlations with the perceptual similarity model.

Representations of visual features and their relationship to behaviour

In a final set of analyses, we assessed how specific visual features and their associated neural codes related to behaviour. To assess perceptual similarity of the stimuli, a separate group of 530 participants completed 500 trials in an online experiment. In each trial, participants were shown three stimuli and were asked to choose the stimulus that looks the most different (i.e., the odd-one out; Figure 1C), and across 265,000 participant trials of various stimulus combinations, we quantified perceptual similarity of stimulus pairs. We used the Representational Similarity Analysis (RSA) framework (Kriegeskorte and Kievit, 2013) to compare neural dissimilarity across different stimuli with dissimilarities computed from visual feature models and behaviour. Neural dissimilarity matrices were constructed using pairwise decoding for all pair combinations of the stimuli, resulting in a symmetrical 256 × 256 matrix for each time point (32640 unique values). Analogous models were constructed for each of the four visual features (contrast, colour, spatial frequency, and orientation) based on the rank similarity of that feature in the stimulus set; importantly, these feature models were orthogonal, with no reliable correlations between them (Figure 5A). Behavioural dissimilarity matrices were constructed from the results of the odd-one-out task (Figure 1C), where higher dissimilarity indicated pairs of stimuli where one of the stimuli tended to be chosen as the odd-one-out when they were presented in triplets together. Figure 5B shows a 2-dimensional embedding of the perceptual dissimilarity between stimuli.

We observed interesting relationships between the neural, feature, and behavioural models. First, we assessed whether visual feature differences were reflected in behaviour (Figure 5A). There were particularly high correlations between behaviour and models of spatial frequency ($r = .567$, $p < .001$) and colour ($r = .497$, $p < .001$). Lower, but still reliable correlations were observed between behaviour and contrast, ($r = .118$, $p < .001$), and behaviour and orientation, ($r = .054$, $p < .001$), indicating that all four feature dimensions were likely being used to assess perceptual similarity of the stimuli. Thus, stimuli that were more similar in terms of spatial frequency, colour, contrast, and orientation tended to be perceived as more similar overall. We then assessed how the neural models related to the feature models and behaviour (Figure 5C). There were high correlations between neural and perceptual similarity from very early stages of processing (onset = 80ms), indicating that early visual responses, rather than purely high-level representations, were relevant for behaviour. The same trend was observed for the 6.67 Hz and 20 Hz presentation rates. Importantly, the neural-perceptual correlation remained for hundreds of milliseconds, suggesting that prolonged neural feature representations are useful and important for perception.

Discussion

Even the most complex processes underlying visual recognition rely on computations of basic visual features such as orientation and spatial frequency. Yet, we still know very little about interactions between features, and their relationship to behaviour. In this study, we investigated how visual features are coded in the brain using a large stimulus set designed to parametrically vary on features of orientation, spatial

frequency, colour and contrast values. With fast image presentation, EEG, and multivariate decoding, we found that these features were processed in parallel in the brain, but varied in the strength and time of maximum coding. Stimulus presentation speed was varied to differentially limit visual processing (Robinson et al., 2019), which showed that image masking influenced the strength but not dynamics (e.g., peak times) of feature information, indicating a particularly robust mechanism for visual feature coding. Further, we show that two-feature interactions and conjunctions are not all coded equally, implying separable neuronal populations are involved for interactions between different features. Behavioural similarity judgements of these stimuli relied on all four features and correlated with neural information from early stages of processing, yet was sustained for hundreds of milliseconds. Together, these results indicate that the earliest visual feature processes contribute to perceptual experience, but that prolonged representations of an image's constituent features are relevant and important for robust perception.

The time course of multiple simple features

Information about orientation, spatial frequency, colour, and contrast was represented in parallel, but with different dynamics, indicating that at least partially separable neural populations are responsible for coding these features. Our results were consistent with previous work, for example showing colour (Hermann et al., 2022; Rosenthal et al., 2020; Teichmann et al., 2020), spatial frequency (Ramkumar et al., 2013), and orientation information (e.g., Moerel et al., 2022b; Pantazis et al., 2018) can be decoded from high temporal resolution neural signals in humans. Going further than previous studies, we were able to show how multiple features of the same stimulus are coded simultaneously and sustained for prolonged periods. This prolonged coding of each feature support prior research showing feature coding in multiple areas of the visual pathway beyond V1 (e.g., Desimone et al., 1985; Groen et al., 2022; Kamitani and Tong, 2005; Marquardt et al., 2018; Seymour et al., 2009). We found distinct representations for each feature, reflecting separable neural populations and/or different codes of multiplexing cells specialised for coding each feature. Time of peak coding, in particular, indicates the stage of processing at which the highest amount of feature-specific information is coded, shedding light on the representations of different features in the visual system. Coding of contrast peaked earlier than the other features, supporting its role as a modulator of other feature coding (Butler et al., 2020), whereas spatial frequency and colour peaked slightly later, and orientation coding was later again. This is consistent with previous work showing later decoding for orientation than spatial frequency (Ramkumar et al., 2013).

Coding of each feature exhibited a pronounced double-peak response, with the first peak around 90-130ms and a smaller second peak around 160-200ms, which corresponded with two distinct stages in the time generalisation analyses. These times are associated with the C1/P100 and N1/N170 event-related potential components, which are typically described as two different stages of visual processing, likely reflecting low-level versus high-level (i.e., face/word/object) image discrimination, respectively (Bentin et al., 1996; Hillyard and Anllo-Vento, 1998). Previous studies using EEG decoding have shown a multi-peak curve for orientation (Moerel et al., 2022b) and object decoding (Grootswagers et al., 2019a; Moerel

et al., 2022a; Robinson et al., 2019), though interestingly decoding curves from magnetoencephalography (MEG) data do not seem to show pronounced second peaks for orientation (Pantazis et al., 2018), spatial frequency (Ramkumar et al., 2013), colour (Hermann et al., 2022; Teichmann et al., 2020, 2019) or object information (Carlson et al., 2013; Cichy et al., 2014; Mohsenzadeh et al., 2018). This points to the second peak in EEG reflecting neural responses from radial dipoles that are difficult to measure with MEG. One potential explanation is that the second peak reflects feedback or recurrent processes. Alpha oscillations have been implicated in feedback-related coherent visual processing (Chen et al., 2023) and notably, frontal alpha and theta oscillations are difficult to measure using MEG (Srinivasan et al., 2006). This could reflect a role of frontal oscillatory activity in high level visual representations after 150ms, in a potential feedback process. Together, the two-stage process for feature distinctions we observed might therefore indicate two sweeps of information; one that is primary feedforward, and one that is primarily feedback (Goddard et al., 2016). This could play into why we (and others) found below-chance classification accuracy for generalisation between different stages of processing: a reversal of information flow might correspond with a reversal of neural information patterns such that images that have stronger feedforward representations might result in weaker feedback information.

Early visual cortex responses are unaffected by changes in presentation rate

Neural dynamics were highly replicable across two different presentation rates (6.67Hz and 20Hz, with the same image duration), showing feature coding is reliable even with limited processing time. This is not surprising given that feature coding relies on early visual cortex which has rapid temporal tuning, and temporal resolution decreases across the visual hierarchy (Groen et al., 2022; Ubaldi and Fairhall, 2021). While we observed small differences for onset times and peak strengths between the 20Hz and 6.67Hz conditions, we do not consider this strong evidence for delays in neural coding because these measures can be influenced by overall signal-to-noise ratio (Grootswagers et al., 2017; Isik et al., 2014). Therefore, given the same peak times and overall dynamics, we consider feature coding unaffected by presentation rate. This is in stark contrast to previous work that used RSVP and decoding, which reported strong effects of presentation rates on decoding accuracies for object stimuli (Grootswagers et al., 2019a, 2019b; Moerel et al., 2022b; Robinson et al., 2019; Shatek et al., 2022). This is likely because the features investigated in this study predominantly rely on feedforward coding in the early visual cortex, whereas the object identities decoded in previous studies rely on the ventral temporal cortex which requires more recurrent processing and is therefore more affected by the masking in fast RSVP. Together, these results demonstrate that feedforward neural processing is highly robust to masking.

Prolonged feature coding and cascading processes in early visual regions

Despite the likely reliance on early visual regions, stimulus feature coding was evident for prolonged periods of time. We found, for example, that spatial frequency and contrast could be decoded from ~70-500 ms in the 6.67Hz condition and from ~100-300 in the 20Hz condition, even though stimuli were only

presented for one frame, 16.66 ms, and were irrelevant to the fixation detection task. This prolonged coding has two implications: cascading processes and temporal overlap. The current study replicated the temporal overlap observed in previous studies, where successive events can be decoded even though their neural processing signals overlap in time (Grootswagers et al., 2019a; King and Wyart, 2021). Here, we found that information about approximately three stimuli could be extracted from the neural signal simultaneously. Importantly, however, simultaneously processed stimuli seem to be held at different processing stages, which highlights potential mechanisms for the brain to accommodate for delays in processing and to keep track of time (cf. Hogendoorn, 2022). The other implication of prolonged information coding is that initial neural responses in early visual areas trigger a robust processing cascade. Despite very brief image presentations, characteristic coding dynamics were observed for each feature, involving at least two distinct stages of processing. The feature-specific nature of this coding is also interesting: rather than initial feature coding that transforms into a more feature-invariant "object" code, later processes still contain feature-specific information about multiple visual features. This suggests that high-level processing relies on maintaining feature information through recurrence.

Relatively weak decoding of orientation

Oriented gratings have for decades been reliably and strongly decoded from fMRI data (Kamitani and Tong, 2005). It is notable that in our study, orientation decoding was relatively low (albeit reliable) compared to other visual features. Previous work similarly reported low orientation decoding accuracy in EEG (e.g. Moerel et al., 2022b), but higher in MEG (Cichy et al., 2015; Pantazis et al., 2018). All these studies used gratings with randomised phase, as we did, so variations in phase cannot explain our low orientation decoding accuracies. Furthermore, our design was very highly powered, with 40 repetitions of all 256 stimuli resulting in 10240 events for each presentation rate and 2560 repetitions per orientation angle. Notably, we did not include cardinal or oblique orientations in our stimulus set, which likely reduced our power in detecting differences between orientations (Pantazis et al., 2018). It could be that the neural populations distinguishing between colour, contrast, and SF are more distributed, with asymmetries in their absolute signal strength (e.g., high contrast drives stronger responses (Albrecht and Hamilton, 1982)), which would make their respective sources easier to distinguish at the scalp. However, at the level of perceptual experience, robust object perception needs to be invariant to rotation to some extent (Karimi-Rouzbahani et al., 2017; Moerel et al., 2022a). Orientation differences could be interpreted as a rotation of the same object, which would reduce its importance in our perceptual similarity task. While local orientation detection is crucial to find edges and shapes, at a higher-level orientation may not be as important, which could account for its weaker decoding compared to other features.

Reliable coding of feature interactions

Feature interactions can shed light on the overlapping nature of neural populations coding for individual features. We assessed these interactions, by looking at how feature coding varied as a function

of the other features. We found several interesting interactions, for example that colour coding decreased as spatial frequency decreased, and vice versa: spatial frequency coding changed across the experimental colours. In light of behavioural results showing that humans tend to perceive mixtures of colours at high spatial frequencies but separable colours at low spatial frequencies (Gegenfurtner and Kiper, 2003), these results point to higher overlap in neural populations coding for colour and high spatial frequency compared with low spatial frequency information. We also found a decrease in contrast coding with decreasing spatial frequencies, and complementary decrease in spatial frequency coding with decreasing contrast. These results fit well with the larger history of perceptual interactions documented in the psychophysics literature focused on contrast sensitivity functions, where spatial frequency sensitivity varies across contrast (Campbell and Robson, 1968). We found no reliable interactions between orientation and other features, possibly because orientation decoding was low in general, though it was consistently above chance. Notably, interactions were not exclusively bidirectional. So, for example, contrast coding varied across colour, but colour decoding was not influenced by contrast, a result that indicates a difference in the modulatory role of each feature. These interaction results were highly reliable across the two presentation rates. The interactions we observed point to partially overlapping neural populations responsible for coding different features.

Separable neural processes for conjunction coding

The brain needs to bind different types of features to form a single percept, yet the neural mechanisms underlying feature conjunctions have remained elusive. In an effort to understand how feature conjunctions are coded, we implemented a novel set of analyses to extract information about conjunctions of two features from the neural signal, by comparing sets of stimuli that were identical in terms of their basic features, but differed in the combinations of these features. The logic of these analyses was similar to those implemented in previous work of colour and motion (Seymour et al., 2009), and colour and form (Taylor and Xu, 2022). Importantly, above-chance decoding in these analyses indicates evidence of feature conjunction coding for a given pair of features. We found reliable decoding of most conjunctions, indicating a transitory stage from individual feature coding to processing higher order visual attributes (e.g., texture, shape). Conjunction coding was typically later than individual feature processing, indicating distinct neural populations from those involved in individual feature processing. Even when taking into account that lower overall classification can lead to later calculated onsets (Grootswagers et al., 2017), the observed dynamics and peaks for the conjunction analyses looked notably different from the single feature analyses, supporting different mechanisms and neural populations for coding conjunctions than for individual feature processing. Interestingly, previous work has found colour conjunction coding in V1-V3 (Seymour et al., 2009; Taylor and Xu, 2022), which was interpreted as “early” feature conjunctions, yet here we find that conjunction coding occurred later than individual feature coding. This delay points to an important role for recurrence and feedback within early visual regions for perception.

The dynamics of conjunction decoding can give insight into the processes underlying feature coding. Conjunction coding was shorter than that for individual features, which could signify a transitory phase to processing conjunctions of more than two features. Crucially, individual feature coding was maintained during conjunction coding, indicating that ongoing single feature processing might be necessary for computations of conjunctions between features. Different dynamics across different 2-way conjunctions suggest different mechanisms for binding different features. These findings support previous research demonstrating a transition from feature to conjunction coding throughout the visual cortex (Cowell et al., 2017). Yet, the maintained feature coding suggests that there is not a clear transformation in processing from feature coding to conjunction coding, as previously thought, and rather suggests that there is a complex interplay between recurrent and feedback processes within different regions specialised for different mechanisms. Although conjunctions of more than two features were too complex to investigate here, these results lay the foundation for future work into more complex feature conjunction coding in the brain.

Feature processing and perceptual experience

An important missing piece of the visual perception puzzle is the extent to which the neural coding of basic visual features contribute to behaviour. Unpacking this relationship allows us to understand how perceptual processing leads to perceptual experience. Our large 4-dimensional stimulus set presents an interesting challenge for assessing behaviour. As an overall judgement of perception, we had participants make "odd-one-out" choices for three simultaneously presented images, allowing choices to be made on any of the four features in each stimulus or some combination of features. Previous work has used the odd-one-out triplet task to great effect in finding the dimensions underlying similarities in a large stimulus set (Hebart et al., 2020). In our case the underlying dimensions were known, which allows us to estimate the weight people give to each dimension. Interestingly, we found that all four features contributed to behaviour to varying levels. Stimulus orientation, contrast, spatial frequency, and colour models each correlated with behavioural similarity ratings, indicating that behaviour was based on a complex weighting of the different features by which the stimuli varied. One interesting finding in the behaviour is that orientation seemed to be the poorest predictor of perceptual similarity, echoing poorer classification for orientation relative to the other features. Spatial frequency and colour accounted for the most variance in behaviour. The emergence of a multi-dimensional space using such a simple behavioural measure supports the validity of the triplet approach for higher level vision (Hebart et al., 2020), and shows how powerful a simple approach can be.

The richness of our behavioural results was also evident by its relationship to measured neural responses evoked by the same stimuli. Previous work has shown that perceptual similarity correlates with neural responses (e.g., Bankson et al., 2018; Cichy et al., 2019), even to the point that behaviour can explain the most variance in neural responses (e.g., Bankson et al., 2018; Contini et al., 2020; Grootswagers

et al., 2022; Mur et al., 2013; Wardle et al., 2016), indicating that perceptual decision-making might be based on a direct behavioural read out of the patterns of stimulus-based neural responses. Here we found that the perceptual similarity yielded reliable correlations with neural responses to the stimuli from very early stages of processing, only 80ms after image presentation. In our study, early neural responses were therefore highly reflective of behaviour. The reliable early correlations are particularly notable given our large stimulus set, which meant that rank-order correlations between neural and perceptual similarity were performed on 32640 pairwise dissimilarity values. Further, our stimuli all had identical retinotopic projections, meaning large position-based neural differences could not contribute to the neural-perceptual relationship as it could in previous work (Bankson et al., 2018; Contini et al., 2020; Wardle et al., 2016). Overall, early and prolonged correlations between neural patterns of activity and perceptual experience points to the basic features of orientation, colour, spatial frequency, and contrast being primary contributors to the perceived form of our simple experimental stimuli.

Methods

Raw and preprocessed data are available online through openneuro: https://openneuro.org/datasets/ds004357. Supplementary Material and analysis scripts are available on github: https://github.com/Tijl/features-eeg

Participants

There were 16 participants (11 female, 5 male, age range 18-27 years) for the electroencephalography (EEG) experiment recruited through the University of Sydney in return for course credit or payment. There were 530 participants for the online behavioural experiment, recruited via SONA in return for course credit. The study was approved by the University of Sydney ethics committee and informed consent was obtained from all participants.

Stimuli

Stimuli were 256 oriented gratings that varied across four feature dimensions: colour, spatial frequency, contrast, and orientation (Figure 1A). The stimuli were 256 × 256 pixel sinusoidal patches with a circular mask constructed using GratingStim in PsychoPy (Peirce et al., 2019) with specified orientations, colours, spatial frequencies and contrast. There were four levels of each feature dimension. The four colours were RGB values [66, 10, 104; 147, 38, 103; 221, 81, 58; 252, 165, 10], approximately equidistant in colour space, and each was presented with their complementary colour as implemented in PsychoPy. Orientations were 22.5, 67.5, 112.5 and 157.5 degrees, circularly spaced. Spatial frequencies were 2.17, 1.58, 0.98, 0.39 cycles per degree, and contrast was .9, .7, .5 and .3, both linearly spaced. The experimental stimuli consisted of all 256 possible combinations of the features (4 orientations × 4 spatial frequencies × 4 colours × 4 contrast levels). Note that the levels of each feature were designed to be approximately equidistant in stimulus space, but these do not necessarily reflect equidistant neural or

perceptual responses; our focus was to include a range of stimuli that varied along four feature dimensions: equally spaced sampling of the dimensions was not crucial to estimate featural dynamics. To avoid phase-related effects, the phase of the stimulus gratings varied randomly on each presentation in the EEG experiment. For the behavioural experiment, a specific (but randomly chosen) phase was used for each stimulus. Phases used in the behavioural experiment are shown in Figure 1.

Online behavioural experiment

Behavioural similarity judgements were collected using an online behavioural experiment (Grootswagers, 2020), programmed in jsPsych (De Leeuw, 2015) and hosted using Jatos (Lange et al., 2015). The experiment involved the display of three stimuli, and participants were asked to select the odd one out. This design has been used previously to yield high quality similarity spaces (Hebart et al., 2020). In total, 530 participants performed 500 trials each, yielding a total of 265,000 similarity judgements. To create a behavioural dissimilarity matrix, the similarity of a pair of stimuli was computed as the number of trials where the pair was presented together but not chosen as the odd one out, divided by the total number of trials that included the pair. The similarity scores were then converted into dissimilarity scores by taking 1 minus the similarity scores.

EEG experiment

Neural responses were collected using electroencephalography (EEG) while participants viewed the experimental stimuli and performed an orthogonal task (Figure 1B). Participants viewed the 60 Hz experimental monitor from approximately 57cm away. Images were presented centrally at 6.5 × 6.5 degrees of visual angle. They were each presented for 16.67 ms duration, in sequences at 6.67Hz (150 ms SOA) and 20Hz (50 ms SOA; Figure 1B). Each sequence consisted of all 256 stimuli presented in random order. There were 80 sequences across the whole experiment, with each stimulus presented 40 times per frequency condition. Participants were asked to fixate on a black bullseye which was presented one second before the sequence began and superimposed on top of all stimuli. The task was to detect when the fixation bullseye changed to a filled circle target and respond using a button press. Targets occurred 2-4 times per sequence.

EEG recording and preprocessing

Continuous neural data were collected using a 128-channel BrainVision ActiChamp EEG system using the international five percent system for electrode placement over the scalp (Oostenveld and Praamstra, 2001). Data were online referenced to FCz and digitised at 1000 Hz. All preprocessing was performed offline using EEGLAB (Delorme and Makeig, 2004). Basic processing was performed: data were filtered using 0.1 Hz high pass and 100 Hz low pass filters, and subsequently downsampled to 250 Hz. Epochs were constructed from 100ms prior to 600ms after each image presentation. No electrode interpolation or artefact rejection was performed (cf. Delorme, 2023).

Analyses

Stimulus feature decoding

Time-resolved multivariate pattern (decoding) analyses (Grootswagers et al., 2017) were performed to determine the temporal dynamics of visual feature coding in the brain. We decoded the EEG channel voltages across the 128 electrodes using CoSMoMVPA (Oosterhof et al., 2016) in MATLAB. For each time point, data were pooled across all electrodes, and we tested whether a classifier could discriminate between patterns of neural activity in response to different stimulus orientations, spatial frequencies, colours, and contrast levels. Regularised linear discriminant analysis (LDA) classifiers were used to decode neural responses to the four levels of each stimulus feature (e.g., stimulus contrast 0.9 vs 0.7 vs 0.5 vs 0.3). Classification was performed separately for each feature, time point, and image presentation rate. A leave-one-sequence-out cross-validation approach was used, where the classifier was trained on trials from all but one sequence (39) and tested on the left-out sequence (1), and this was repeated 40 times so each sequence was the test set once. Each sequence contained 256 stimuli, with a quarter of these belonging to each stimulus feature level. Thus, each feature analysis contained the same trials, but in different combinations. Decoding accuracy was calculated as the proportion of correct cross-validated classifier predictions and compared to chance performance of 0.25.

Feature interactions

To assess how coding of different features interact, we performed the same time-resolved decoding analyses using subsets of the data corresponding with specific stimulus features. We classified each of the four stimulus features for each level of the remaining three features; for example, decoding stimulus orientation for each level of contrast, spatial frequency, and colour. The same decoding scheme (i.e., 4 class, leave-one-sequence-out cross-validation) was used as in the original feature decoding analysis, but with only one quarter of the trials. Thus, chance level was still 0.25. To compare across conditions, we assessed peak decoding accuracy during a 20ms time window centred on the peak of the original feature analysis (i.e., 120ms for orientation, 112ms for SF, 112ms for colour and 96ms for contrast). The mean accuracy was calculated for each time window per participant and statistically compared across levels of a given feature (Figure 3).

Feature conjunctions

To assess the conjunctions of pairs of features (e.g., SF × orientation), we decoded groups of stimuli that each had the same absolute features, but varied in their feature *combinations* (see Figure 4). For example, low spatial frequency high contrast stimuli and high spatial frequency low contrast stimuli (class 1) versus low spatial frequency low contrast and high spatial frequency high contrast stimuli (class 2). For each pair of features, classification was performed for the 36 different possible stimulus combinations (e.g., SF3ori3/SF2ori2 vs SF3ori2/SF2ori3, SF3ori3/SF2ori4 vs SF3ori4/SF2ori3, etc) and then the mean

was calculated. Above chance classification for this analysis reflects neural responses to the combinations of different pairs of features, indicating the coding of feature *conjunctions*. Note that this analysis requires a classifier to pick up on features that reflect differences between a group of two stimuli versus another two stimuli, but this does not mean that it is necessarily using features that are common within each group; instead, we expect that a classifier learns neural patterns associated with each of the four stimuli and can find a boundary that separates two stimuli from two others. This analysis is very similar to previous analyses on colour-form conjunctions (Taylor and Xu, 2022).

Representational similarity analyses

To assess relationships between the neural, behavioural and feature models, we used the Representational Similarity Analysis framework (Kriegeskorte and Kievit, 2013). Neural representational dissimilarity matrices were constructed using pairwise decoding for all pair combinations of the stimuli, resulting in a symmetrical 256 × 256 matrix for each time point per participant. Model dissimilarity matrices were constructed for each of the four visual features (contrast, colour, spatial frequency, and orientation) based on the rank similarity of that feature in the stimulus set (Figure 5A). For the contrast model, for example, stimuli that were presented at contrast level 0.9 were most similar to level 0.7 (dissimilarity = 1), more dissimilar to level 0.5 (dissimilarity = 2) and most dissimilar to level 0.3 (dissimilarity = 3). The same scheme was used for spatial frequency and colour. Due to the circular nature of orientation, the orientation model was slightly different; stimuli orientated at 22.5 degrees were as similar to 67.5 degrees (45 degree difference; dissimilarity = 1) as they were to 157.5(-22.5) degrees (45 degrees difference; dissimilarity = 1). Importantly, each of the four feature models were orthogonal (orientation versus other models r = -.008, p = .171; the others r = -.007, p = .189). Finally, behavioural dissimilarity matrices were constructed from the results of the odd-one-out task, where higher dissimilarity indicated pairs of stimuli where one of the stimuli tended to be chosen as the odd-one-out when they were presented together (Figure 5B).

To assess how visual features of the stimuli relate to behavioural responses of their similarity, we correlated the behavioural results with each of the four feature models. Then, to assess how stimulus features and behavioural judgements are related to the neural responses of the stimuli, we correlated the neural dissimilarity matrices with the four feature models and the behavioural model, separately for each time point and participant. Each comparison was performed using Spearman correlation for the unique values in the dissimilarity matrices (i.e., the lower triangles, 32640 values), yielding a very robust estimate of the relationship between each model.

Statistical inference

To statistically compare group-level decoding accuracies or correlations to chance level, we used Bayes factors (Morey and Rouder, 2011; Rouder et al., 2009; Teichmann et al., 2022), as implemented in the Bayesfactor R package (Morey and Rouder, 2018) and its corresponding implementation for time-series

neuroimaging data (Teichmann et al., 2022). The prior for the null-hypothesis was set at chance level (for decoding) or zero (for the correlations). The alternative hypothesis prior was an interval ranging from small effect sizes to infinity, accounting for small above-chance results as a result of noise (Morey and Rouder, 2011; Teichmann et al., 2022). For calculating the onset of above chance decoding or correlations, we found the first three consecutive time points where all Bayes Factors were >10. To be able to compare onset and peak times, we calculated 95% confidence intervals by using a leave-two-participants-out jackknifing approach, where we calculated the onset and peak for all possible leave-two-out permutations (n=120 permutations for 16 participants), and took the 95th percentile of the resulting distributions.

Acknowledgements

This work was supported by an Australian Research Council (ARC) Discovery Early Career Researcher Awards awarded to TG (DE230100380) and AKR (DE200101159), and ARC Discovery Projects awarded to TAC (DP160101300 and DP200101787). SMS was supported by an Australian Government research Training Program Scholarship. The authors acknowledge the Sydney Informatics Hub and the University of Sydney's high performance computing cluster Artemis for providing the high-performance computing resources that contributed to these research results.

Author contributions

Conceptualization (TG,AKR); Methodology (TG,AKR); Investigation (TG,AKR,SMS); Formal analysis (TG,AKR,SMS); Data Curation (TG); Visualization (TG,AKR); Writing - Original Draft (TG,AKR); Writing - Review & Editing (TG,AKR,SMS,TC); Supervision (TC); Funding acquisition (AKR,TC)

References

Albrecht, D.G., Hamilton, D.B., 1982. Striate cortex of monkey and cat: contrast response function. J. Neurophysiol. 48, 217–237. https://doi.org/10.1152/jn.1982.48.1.217

Bankson, B.B., Hebart, M.N., Groen, I.I.A., Baker, C.I., 2018. The temporal evolution of conceptual object representations revealed through models of behavior, semantics and deep neural networks. NeuroImage 178, 172–182. https://doi.org/10.1016/j.neuroimage.2018.05.037

Bentin, S., Allison, T., Puce, A., Perez, E., McCarthy, G., 1996. Electrophysiological Studies of Face Perception in Humans. J. Cogn. Neurosci. 8, 551–565. https://doi.org/10.1162/jocn.1996.8.6.551

Brouwer, G.J., Heeger, D.J., 2009. Decoding and Reconstructing Color from Responses in Human Visual Cortex. J. Neurosci. 29, 13992–14003. https://doi.org/10.1523/JNEUROSCI.3577-09.2009

Butler, R., Mierzwinski, G.W., Bernier, P.M., Descoteaux, M., Gilbert, G., Whittingstall, K., 2020. Neurophysiological basis of contrast dependent BOLD orientation tuning. NeuroImage 206, 116323. https://doi.org/10.1016/j.neuroimage.2019.116323

Campbell, F.W., Robson, J.G., 1968. Application of fourier analysis to the visibility of gratings. J. Physiol. 197, 551–566.

Carlson, T.A., Ritchie, J.B., Kriegeskorte, N., Durvasula, S., Ma, J., 2014. Reaction Time for Object Categorization Is Predicted by Representational Distance. J. Cogn. Neurosci. 26, 132–142. https://doi.org/10.1162/jocn_a_00476

Carlson, T.A., Tovar, D.A., Alink, A., Kriegeskorte, N., 2013. Representational dynamics of object vision: The first 1000 ms. J. Vis. 13, 1. https://doi.org/10.1167/13.10.1

Chen, L., Cichy, R.M., Kaiser, D., 2023. Alpha-frequency feedback to early visual cortex orchestrates coherent natural vision. https://doi.org/10.1101/2023.02.10.527986

Cichy, R.M., Kriegeskorte, N., Jozwik, K.M., van den Bosch, J.J.F., Charest, I., 2019. The spatiotemporal neural dynamics underlying perceived similarity for real-world objects. NeuroImage 194, 12–24. https://doi.org/10.1016/j.neuroimage.2019.03.031

Cichy, R.M., Pantazis, D., 2017. Multivariate pattern analysis of MEG and EEG: A comparison of representational structure in time and space. NeuroImage 158, 441–454. https://doi.org/10.1016/j.neuroimage.2017.07.023

Cichy, R.M., Pantazis, D., Oliva, A., 2014. Resolving human object recognition in space and time. Nat. Neurosci. 17, 455–462. https://doi.org/10.1038/nn.3635

Cichy, R.M., Ramirez, F.M., Pantazis, D., 2015. Can visual information encoded in cortical columns be decoded from magnetoencephalography data in humans? NeuroImage 121, 193–204. https://doi.org/10.1016/j.neuroimage.2015.07.011

Contini, E.W., Goddard, E., Grootswagers, T., Williams, M., Carlson, T., 2020. A humanness dimension to visual object coding in the brain. NeuroImage 221, 117139. https://doi.org/10.1016/j.neuroimage.2020.117139

Cowell, R.A., Leger, K.R., Serences, J.T., 2017. Feature-coding transitions to conjunction-coding with progression through human visual cortex. J. Neurophysiol. 118, 3194–3214. https://doi.org/10.1152/jn.00503.2017

De Leeuw, J.R., 2015. jsPsych: A JavaScript library for creating behavioral experiments in a Web browser. Behav. Res. Methods 47, 1–12.

Delorme, A., 2023. EEG is better left alone. Sci. Rep. 13, 2372. https://doi.org/10.1038/s41598-023-27528-0

Delorme, A., Makeig, S., 2004. EEGLAB: an open source toolbox for analysis of single-trial EEG dynamics including independent component analysis. J. Neurosci. Methods 134, 9–21. https://doi.org/10.1016/j.jneumeth.2003.10.009

Desimone, R., Schein, S.J., Moran, J., Ungerleider, L.G., 1985. Contour, color and shape analysis beyond the striate cortex. Vision Res., Neural Basis of Visual PerceptionProceedings of the 6th Taniguchi International Symposium on Visual Science 25, 441–452. https://doi.org/10.1016/0042-6989(85)90069-0

Friedman, H.S., Zhou, H., von der Heydt, R., 2003. The coding of uniform colour figures in monkey visual cortex. J. Physiol. 548, 593–613. https://doi.org/10.1111/j.1469-7793.2003.00593.x

Gegenfurtner, K.R., Kiper, D.C., 2003. Color Vision. Annu. Rev. Neurosci. 26, 181–206. https://doi.org/10.1146/annurev.neuro.26.041002.131116

Goddard, E., Carlson, T.A., Dermody, N., Woolgar, A., 2016. Representational dynamics of object recognition: Feedforward and feedback information flows. NeuroImage 128, 385–397. https://doi.org/10.1016/j.neuroimage.2016.01.006

Groen, I.I.A., Piantoni, G., Montenegro, S., Flinker, A., Devore, S., Devinsky, O., Doyle, W., Dugan, P., Friedman, D., Ramsey, N.F., Petridou, N., Winawer, J., 2022. Temporal Dynamics of Neural Responses in Human Visual Cortex. J. Neurosci. 42, 7562–7580. https://doi.org/10.1523/JNEUROSCI.1812-21.2022

Grootswagers, T., 2020. A primer on running human behavioural experiments online. Behav. Res. Methods 52, 2283–2286. https://doi.org/10.3758/s13428-020-01395-3

649 Grootswagers, T., Cichy, R.M., Carlson, T.A., 2018. Finding decodable information that can be read out
650 in behaviour. NeuroImage 179, 252–262. https://doi.org/10.1016/j.neuroimage.2018.06.022
651 Grootswagers, T., McKay, H., Varlet, M., 2022. Unique contributions of perceptual and conceptual
652 humanness to object representations in the human brain. NeuroImage 257, 119350.
653 https://doi.org/10.1016/j.neuroimage.2022.119350
654 Grootswagers, T., Robinson, A.K., Carlson, T.A., 2019a. The representational dynamics of visual objects
655 in rapid serial visual processing streams. NeuroImage 188, 668–679.
656 https://doi.org/10.1016/j.neuroimage.2018.12.046
657 Grootswagers, T., Robinson, A.K., Shatek, S.M., Carlson, T.A., 2019b. Untangling featural and
658 conceptual object representations. NeuroImage 202, 116083.
659 https://doi.org/10.1016/j.neuroimage.2019.116083
660 Grootswagers, T., Wardle, S.G., Carlson, T.A., 2017. Decoding Dynamic Brain Patterns from Evoked
661 Responses: A Tutorial on Multivariate Pattern Analysis Applied to Time Series Neuroimaging
662 Data. J. Cogn. Neurosci. 29, 677–697. https://doi.org/10.1162/jocn_a_01068
663 Hajonides, J.E., Nobre, A.C., van Ede, F., Stokes, M.G., 2021. Decoding visual colour from scalp
664 electroencephalography measurements. NeuroImage 237, 118030.
665 https://doi.org/10.1016/j.neuroimage.2021.118030
666 Hebart, M.N., Zheng, C.Y., Pereira, F., Baker, C.I., 2020. Revealing the multidimensional mental
667 representations of natural objects underlying human similarity judgements. Nat. Hum. Behav. 4,
668 1173–1185. https://doi.org/10.1038/s41562-020-00951-3
669 Hermann, K.L., Singh, S.R., Rosenthal, I.A., Pantazis, D., Conway, B.R., 2022. Temporal dynamics of
670 the neural representation of hue and luminance polarity. Nat. Commun. 13, 661.
671 https://doi.org/10.1038/s41467-022-28249-0
672 Hillyard, S.A., Anllo-Vento, L., 1998. Event-related brain potentials in the study of visual
673 selective attention. Proc. Natl. Acad. Sci. 95, 781–787. https://doi.org/10.1073/pnas.95.3.781
674 Hogendoorn, H., 2022. Perception in real-time: predicting the present, reconstructing the past. Trends
675 Cogn. Sci. 26, 128–141. https://doi.org/10.1016/j.tics.2021.11.003
676 Hubel, D.H., 1988. Eye, Brain and Vision, volume 22 of Scientific American Library. Sci. Am. Press N.
677 Y.
678 Hubel, D.H., Wiesel, T.N., 1959. Receptive fields of single neurones in the cat's striate cortex. J. Physiol.
679 148, 574.
680 Isik, L., Meyers, E.M., Leibo, J.Z., Poggio, T., 2014. The dynamics of invariant object recognition in the
681 human visual system. J. Neurophysiol. 111, 91–102. https://doi.org/10.1152/jn.00394.2013
682 Kamitani, Y., Tong, F., 2005. Decoding the visual and subjective contents of the human brain. Nat.
683 Neurosci. 8, 679–685. https://doi.org/10.1038/nn1444
684 Karimi-Rouzbahani, H., Bagheri, N., Ebrahimpour, R., 2017. Hard-wired feed-forward visual mechanisms
685 of the brain compensate for affine variations in object recognition. Neuroscience.
686 https://doi.org/10.1016/j.neuroscience.2017.02.050
687 King, J.-R., Dehaene, S., 2014. Characterizing the dynamics of mental representations: the temporal
688 generalization method. Trends Cogn. Sci. 18, 203–210. https://doi.org/10.1016/j.tics.2014.01.002
689 King, J.-R., Pescetelli, N., Dehaene, S., 2016. Brain mechanisms underlying the brief maintenance of seen
690 and unseen sensory information. Neuron 92, 1122–1134.
691 King, J.-R., Wyart, V., 2021. The Human Brain Encodes a Chronicle of Visual Events at Each Instant
692 of Time Through the Multiplexing of Traveling Waves. J. Neurosci. 41, 7224–7233.
693 https://doi.org/10.1523/JNEUROSCI.2098-20.2021
694 Kriegeskorte, N., Kievit, R.A., 2013. Representational geometry: integrating cognition, computation, and
695 the brain. Trends Cogn. Sci. 17, 401–412. https://doi.org/10.1016/j.tics.2013.06.007

696 Lange, K., Kühn, S., Filevich, E., 2015. "Just Another Tool for Online Studies" (JATOS): An Easy
697 Solution for Setup and Management of Web Servers Supporting Online Studies. PLOS ONE 10,
698 e0130834. https://doi.org/10.1371/journal.pone.0130834
699 Marquardt, I., Schneider, M., Gulban, O.F., Ivanov, D., Uludağ, K., 2018. Cortical depth profiles of
700 luminance contrast responses in human V1 and V2 using 7 T fMRI. Hum. Brain Mapp. 39, 2812–
701 2827. https://doi.org/10.1002/hbm.24042
702 Moerel, D., Grootswagers, T., Robinson, A., Engeler, P., Holcombe, A.O., Carlson, T.A., 2022a. Rotation-
703 tolerant representations elucidate the time-course of high-level object processing.
704 https://doi.org/10.31234/osf.io/wp73u
705 Moerel, D., Grootswagers, T., Robinson, A.K., Shatek, S.M., Woolgar, A., Carlson, T.A., Rich, A.N.,
706 2022b. The time-course of feature-based attention effects dissociated from temporal expectation
707 and target-related processes. Sci. Rep. 12, 6968. https://doi.org/10.1038/s41598-022-10687-x
708 Mohsenzadeh, Y., Qin, S., Cichy, R.M., Pantazis, D., 2018. Ultra-Rapid serial visual presentation reveals
709 dynamics of feedforward and feedback processes in the ventral visual pathway. eLife 7, e36329.
710 https://doi.org/10.7554/eLife.36329
711 Morey, R.D., Rouder, J.N., 2018. BayesFactor: Computation of Bayes Factors for Common Designs.
712 Morey, R.D., Rouder, J.N., 2011. Bayes factor approaches for testing interval null hypotheses. Psychol.
713 Methods 16, 406.
714 Mur, M., Meys, M., Bodurka, J., Goebel, R., Bandettini, P.A., Kriegeskorte, N., 2013. Human Object-
715 Similarity Judgments Reflect and Transcend the Primate-IT Object Representation. Front.
716 Psychol. 4. https://doi.org/10.3389/fpsyg.2013.00128
717 Oostenveld, R., Praamstra, P., 2001. The five percent electrode system for high-resolution EEG and ERP
718 measurements. Clin. Neurophysiol. 112, 713–719. https://doi.org/10.1016/S1388-2457(00)00527-
719 7
720 Oosterhof, N.N., Connolly, A.C., Haxby, J.V., 2016. CoSMoMVPA: Multi-Modal Multivariate Pattern
721 Analysis of Neuroimaging Data in Matlab/GNU Octave. Front. Neuroinformatics 10.
722 https://doi.org/10.3389/fninf.2016.00027
723 Pantazis, D., Fang, M., Qin, S., Mohsenzadeh, Y., Li, Q., Cichy, R.M., 2018. Decoding the orientation of
724 contrast edges from MEG evoked and induced responses. NeuroImage, New advances in encoding
725 and decoding of brain signals 180, 267–279. https://doi.org/10.1016/j.neuroimage.2017.07.022
726 Peirce, J., Gray, J.R., Simpson, S., MacAskill, M., Höchenberger, R., Sogo, H., Kastman, E., Lindeløv,
727 J.K., 2019. PsychoPy2: Experiments in behavior made easy. Behav. Res. Methods 51, 195–203.
728 https://doi.org/10.3758/s13428-018-01193-y
729 Ramkumar, P., Jas, M., Pannasch, S., Hari, R., Parkkonen, L., 2013. Feature-Specific Information
730 Processing Precedes Concerted Activation in Human Visual Cortex. J. Neurosci. 33, 7691–7699.
731 https://doi.org/10.1523/JNEUROSCI.3905-12.2013
732 Ritchie, J.B., Tovar, D.A., Carlson, T.A., 2015. Emerging Object Representations in the Visual System
733 Predict Reaction Times for Categorization. PLoS Comput Biol 11, e1004316.
734 https://doi.org/10.1371/journal.pcbi.1004316
735 Robinson, A.K., Grootswagers, T., Carlson, T.A., 2019. The influence of image masking on object
736 representations during rapid serial visual presentation. NeuroImage 197, 224–231.
737 https://doi.org/10.1016/j.neuroimage.2019.04.050
738 Rosenthal, I.A., Singh, S.R., Hermann, K.L., Pantazis, D., Conway, B.R., 2020. Color Space Geometry
739 Uncovered with Magnetoencephalography. Curr. Biol. https://doi.org/10.1016/j.cub.2020.10.062
740 Rouder, J.N., Speckman, P.L., Sun, D., Morey, R.D., Iverson, G., 2009. Bayesian t tests for accepting
741 and rejecting the null hypothesis. Psychon. Bull. Rev. 16, 225–237.
742 Seymour, K., Clifford, C.W.G., Logothetis, N.K., Bartels, A., 2009. The Coding of Color, Motion, and
743 Their Conjunction in the Human Visual Cortex. Curr. Biol. 19, 177–183.
744 https://doi.org/10.1016/j.cub.2008.12.050

745 Shatek, S.M., Robinson, A.K., Grootswagers, T., Carlson, T.A., 2022. Capacity for movement is an
746 organisational principle in object representations. NeuroImage 261, 119517.
747 https://doi.org/10.1016/j.neuroimage.2022.119517
748 Srinivasan, R., Winter, W.R., Nunez, P.L., 2006. Source analysis of EEG oscillations using high-resolution
749 EEG and MEG, in: Neuper, C., Klimesch, W. (Eds.), Progress in Brain Research, Event-Related
750 Dynamics of Brain Oscillations. Elsevier, pp. 29–42. https://doi.org/10.1016/S0079-
751 6123(06)59003-X
752 Taylor, J., Xu, Y., 2022. Representation of color, form, and their conjunction across the human ventral
753 visual pathway. NeuroImage 251, 118941. https://doi.org/10.1016/j.neuroimage.2022.118941
754 Teichmann, L., Grootswagers, T., Carlson, T.A., Rich, A.N., 2019. Seeing versus knowing: The temporal
755 dynamics of real and implied colour processing in the human brain. NeuroImage 200, 373–381.
756 https://doi.org/10.1016/j.neuroimage.2019.06.062
757 Teichmann, L., Moerel, D., Baker, C., Grootswagers, T., 2022. An empirically-driven guide on using Bayes
758 Factors for M/EEG decoding. Aperture Neuro 1, 1–10. https://www.doi.org/10.52294/82179f90-
759 eeb9-4933-adbe-c2a454577289
760 Teichmann, L., Quek, G.L., Robinson, A.K., Grootswagers, T., Carlson, T.A., Rich, A.N., 2020. The
761 Influence of Object-Color Knowledge on Emerging Object Representations in the Brain. J.
762 Neurosci. 40, 6779–6789. https://doi.org/10.1523/JNEUROSCI.0158-20.2020
763 Ubaldi, S., Fairhall, S.L., 2021. fMRI-Indexed neural temporal tuning reveals the hierarchical organsiation
764 of the face and person selective network. NeuroImage 227, 117690.
765 https://doi.org/10.1016/j.neuroimage.2020.117690
766 Van Essen, D.C., Gallant, J.L., 1994. Neural mechanisms of form and motion processing in the primate
767 visual system. Neuron 13, 1–10.
768 Wardle, S.G., Kriegeskorte, N., Grootswagers, T., Khaligh-Razavi, S.-M., Carlson, T.A., 2016. Perceptual
769 similarity of visual patterns predicts dynamic neural activation patterns measured with MEG.
770 NeuroImage 132, 59–70. https://doi.org/10.1016/j.neuroimage.2016.02.019
771 Zeki, S., 2020. "Multiplexing" cells of the visual cortex and the timing enigma of the binding problem.
772 Eur. J. Neurosci. 52, 4684–4694. https://doi.org/10.1111/ejn.14921
773 Zeki, S., Watson, J.D., Lueck, C.J., Friston, K.J., Kennard, C., Frackowiak, R.S., 1991. A direct
774 demonstration of functional specialization in human visual cortex. J. Neurosci. 11, 641–649.
775